A new class of electron emitters

N. A. Soboleva

All-Union Institute of Scientific and Technical Information (VINITI)

Usp. Fiz. Nauk 111, 331-353 (October, 1973)

This review reflects the status (in early 1973) of the problem of producing photoemitters and secondary and field emitters based on a new principle, that of obtaining semiconductor structures with negative electron affinity (NEA). The energy level scheme of the surface region of a semiconductor with NEA is examined, as well as the conditions for its realization. The main theoretical concepts of the mechanism of the emission from NEA emitters are developed, and the difference between their characteriistics and the corresponding characteristics of ordinary emitters are indicated. The technology is discussed of the production of NEA photocathodes for the visbile and infrared region of the spectrum, based on III-V semiconductor compounds (principally GaAs) and their solid solutions. Aspects of the production of semitransparent NEA photocathodes and secondary emitters operating in transmission are noted. The principal parameters of the experimental and commercial NEA photocathodes and secondary electron emitters are given. Data are reported on the use of surfaces with NEA in field-emission film cathodes, the operating principle of injection and optoelectronic field emission cathodes is described, and their present-day parameters are given.

Practically all of the technical photoemission and secondary-emission materials that have been used up to now in photoelectric devices (vacuum photocells, photomultipliers, electron-optic converters, transmitting television tubes) were discovered in the period from 1930 to 1955 through empirical searches, technological tests, and chance findings. The first attempts to study systematically the properties of emission materials and to develop theoretical views of how they work were undertaken in 1939–1940. These studies were renewed at the end of the forties and intensified, having started to grow anew in connection with the creation of a general theory of semiconductors. These studies, mainly on the photoemission properties of the alkali antimonides, resulted in formulation of the main requirements that efficient emitters of photo- and secondary electrons must satisfy.[1-3]

The process of any non-equilibrium electron emission consists of three stages: 1) excitation, 2) transport to the surface, and 3) escape of the electrons into the vacuum. In photoemission, the first stage is determined by the optical properties of the material, and in secondary emission, by the laws of interaction of fast primary electrons with the solid. The latter stages differ little in photo- and secondary emission.

The transport of excited electrons is usually characterized by the effective escape depth, i.e., the mean distance that they can travel while yet remaining able to escape. The greater the escape depth of the electrons is in comparison with their excitation depth, the more efficient the emitter is. In the usual semiconductor materials, hot electrons participate in emission, and they remain able to be emitted until they dissipate part of their excess energy and are left in an energy level below the vacuum level. The scattering length of hot electrons (which is equal to their escape depth) is determined by the nature of their interaction with the solid. If the electrons can dissipate energy by exciting valence electrons of the semiconductor (i.e., in impact ionization, which is accompanied by generation of electron-hole pairs), then the scattering length does not exceed the mean free path, which is 10–20 Å.

If such interactions are energetically impossible—for photoelectrons excited near the threshold of the photoeffect, they are impossible if the material possesses an electron affinity[1)] smaller than the width of the forbidden band, then the main form of dissipation of energy of hot electrons will be interaction with optical phonons and lattice defects. Then the escape depth of hot electrons depends on their energy, and it can exceed by factors of tens the mean free path, being as much as ~150–300 Å. In fact, even in this most favorable case, the escape depth of hot electrons proves to be substantially less than the depth of optical absorption, especially near the threshold of the photoeffect, where the absorption coefficient is small ($\alpha \sim 10^4$ cm^{-1}; $1/\alpha \sim 1$ μm).

Semiconductors having a small enough electron affinity (at least having $\mathcal{E}_a < \mathcal{E}_g$) and any further decrease in $\mathcal{E}_a$ will improve the transport properties, and thus must improve the emission efficiency of the material. We can say that the electron affinity of semiconductors is the main parameter that determines their emission efficiency.

Figure 1 shows the energy diagrams of the surface regions of semiconductors having p- and n-type conduction. As we see, the bending of the bands at the surface has the result that the effective electron affinity (i.e., the energy spacing from the vacuum level to the bottom of the conduction band in the bulk of the material beyond the narrow band-bending region) declines for p-type semiconductors, but increases for n-type, as compared with weakly-doped semiconductors having flat bands. In addition, since the bands are bent upward in

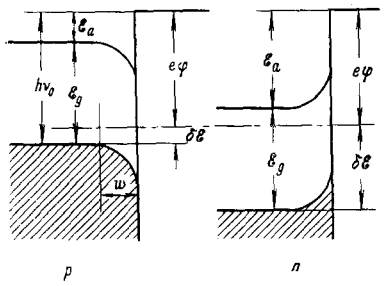

FIG. 1. Energy diagrams of the subsurface region of semiconductors having n- and p-type conduction.

n-type semiconductors, this creates an additional barrier for conduction electrons at the vacuum boundary. Conversely, the bending of the bands in p-type semiconductors favors emission. Hence p-type semiconductors are better emitters than n-type.

As studies have shown, all of the known technical photocathodes that can be classified as "efficient photoemitters" (having quantum yields >0.1 at relatively short distances from the threshold) confirm these ideas: they are semiconductors having low electron affinities and p-type conduction.

The most sensitive of the photocathodes, which belong to the class of $A^{I}B^{V}$ compounds, is a multialkali photocathode of composition K, Na, Cs-Sb. It is characterized by the following parameters: a mean integral sensitivity 200–250 μA/lumen, and in the modern, perfected modification, up to 450 μA/lumen and even 600 μA/lumen with optical amplification using total internal reflection. The peak of the spectral characteristic lies 1.0–1.5 eV from the threshold, and the quantum yield at the peak is as much as 0.2–0.4. The threshold wavelength is as long as 940–960 nm for the best specimens. The quantum yield is 3–4% in the 800 nm region. The thermal current density at room temperature is $\sim 10^{-15}$ A/cm^2.

The secondary-emission properties of materials are also mainly determined by transport of relatively slow secondary electrons, and the conditions that ensure a high secondary-emission coefficient practically coincide with those for high photoemission efficiency, but without the restrictions on optical properties and on the width of the forbidden band. Photomultiplier dynodes are most frequently oxides of magnesium or beryllium and photosensitive Cs_3Sb films. At the peak of the photoemission characteristic (with a primary voltage of 0.8–1 kV), the secondary-emission characteristic of these materials is as great as 10–15.

The formulation of clear-cut ideas on the mechanism of emission by semiconductors has opened the path to purposefully influencing the properties of the materials in order to raise their emission ability. As we see from the abovesaid, they fundamentally amount to developing ways of reducing the electron affinity of semiconductors.

The following evident relationship exists between the photoemission threshold $h\nu_0$ and the work function φ of a semiconductor:

$$h\nu_0 = \mathcal{E}_g + \mathcal{E}_a = e\varphi + \delta\mathcal{E}. \quad (1)$$

Here $\delta\mathcal{E}$ is the energy gap between the top of the valence band and the Fermi level.

We get from Eq. (1)

$$\mathcal{E}_a = e\varphi + \delta\mathcal{E} - \mathcal{E}_g. \quad (2)$$

We can easily see that we should do the following in order to reduce the electron affinity $\mathcal{E}_a$ of a material having a fixed width of forbidden band: a) reduce the work function φ, and b) reduce $\delta\mathcal{E}$. The ways of reducing the work function have been well studied; in order to do this, one coats the surface with a film of electropositive atoms (e.g., cesium) or molecules having a large dipole moment (BaO, CsF, etc.). One can attain the other goal of decreasing $\delta\mathcal{E}$ by doping the semiconductor with an acceptor impurity: the higher the degree of doping, the lower the Fermi level is dropped.

The limiting manifestation of these efforts is to lower the electron affinity to zero or even to a negative value. In order to do this, as we see from (2), we must increase the acceptor concentration to a level such that the Fermi level coincides with the top of the valence band ($\delta\mathcal{E} = 0$). If here we lower the work function at the surface of the semiconductor to a value equal to or less than the width of its forbidden band, we get

$$e\varphi \leqslant \mathcal{E}_g, \quad \mathcal{E}_a = e\varphi - \mathcal{E}_g \leqslant 0. \quad (3)$$

The Dutch physicists Scheer and van Laar[4] first produced a photoemitter having a zero electron affinity in 1965.

To reduce the work function, they used a nearly-monatomic cesium film. When the latter is adsorbed onto a clean surface of a material, the work function of the latter acquires at the minimum a value approximately equal to the ionization energy of the adsorbed cesium atoms (~1.4 eV). Gallium arsenide proved to be the most suitable material for making a photoemitter having zero electron affinity: it has $\mathcal{E}_g = 1.4$ eV, straight bands that make possible high optical absorption near the edge of the intrinsic band, and it easily dissolves an impurity (e.g., Zn) in very high concentration (>10^{19} cm^{-3}). The first photocathode was prepared according to this system from GaAs with a Cs film on a surface cleaned by cleaving a single GaAs crystal in an ultrahigh vacuum. It immediately showed an integral sensitivity of 500 μA/lumen, which exceeded by a factor of two the sensitivity of the most efficient of ordinary photocathodes, and it had a photoemission threshold that coincided with the long-wavelength optical absorption edge ($h\nu_0 = \mathcal{E}_g$).

The absence of a potential barrier at the surface of a semiconductor having zero or negative electron affinity fundamentally changes the nature of emission processes. Figure 2 shows the emission diagrams and the energy distribution of emitted electrons for semiconductors having positive and negative electron affinities. As we see, when there is no potential barrier, not only hot electrons can participate in emission, but also thermalized electrons, i.e., electrons that have dropped to the lower levels of the conduction band. This fundamentally changes the mechanism of transport of the excited electrons: it is converted from transport of

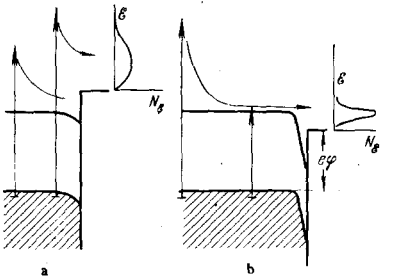

FIG. 2. Diagrams of electron emission from semiconductors having positive (a) and negative (b) electron affinity.

hot electrons into diffusion of minority carriers in the semiconductor.

The lifetime of thermalized electrons, which is governed by recombination, is 10^{-8}–10^{-9} sec for $A^{III}B^{V}$-type semiconductors, and ~10^{-6}–10^{-5} sec for Si. That is, it exceeds by a large factor the time for thermalization of hot electrons (10^{-14}–10^{-12} sec). The escape depth of the photoelectrons coincides with the diffusion length of electrons in the semiconductor, which usually considerably exceeds the escape depth of hot electrons, and it can exceed the optical absorption depth $1/\alpha$ even near the edge of the intrinsic band.

Achievement of a negative electron affinity permits most of the excited photoelectrons to escape into the vacuum, and this leads to very high quantum yields, even in the immediate vicinity of the photoeffect threshold $h\nu_0 = \mathcal{E}_g$.

At high doping levels of the semiconductor, which is one of the conditions for achieving zero electron affinity, the width w of the band-bending region at the surface does not exceed 50–100 Å. Thus, we can assume that all of the radiation is absorbed in the bulk of the semiconductor beyond this region. The electrons that are excited at a distance of the diffusion length from the surface are quickly thermalized. As they diffuse to the surface, they enter the band-bending region. An electric field is concentrated there and accelerates them toward the surface. In the band-bending region, the thermalized electrons again become hot electrons. That is, the mechanism of phonon energy loss acts on them, and reduces their probability of escape. At a high enough concentration of doping impurity, the width of the band-bending region does not exceed substantially the mean free path of the electrons for phonon scattering, and the electrons pass through it with insignificant losses. By lowering the work function to the point of negative electron affinity, one can reduce the "detrimental" part of the band-bending region, i.e., the part of it where the bottom of the conduction band lies below the vacuum level.

The spectral characteristics of photoemitters having negative electron affinity (NEA photoemitters) differ from ordinary photocathodes in their uniformly high quantum yield over a broad spectral range up to the photoemission threshold, which is determined by the width of the forbidden band of the material. That is, they are distinguished by a steep rise in spectral sensitivity near the threshold. NEA emitters of secondary electrons are characterized by considerably higher secondary-emission coefficients for high-energy primary electrons, which penetrate to great depths into the material.

Since most of the excited electrons can thermalize before escaping into the vacuum, NEA emitters, both photo- and secondary emitters, differ from ordinary emitters in their considerably narrower energy spectrum of emitted electrons and smaller mean value of initial energy (as we can see from Fig. 2).

James, Moll, and Spicer[5-7] have developed a quantitative theory of action of NEA photoemitters based on the example of gallium arsenide coated with a film of cesium.

Figure 3 shows a simplified band diagram of GaAs. The optical transitions in this material are direct electronic transitions. That is, they occur with conservation of the wave vector, as shown by the arrows in Fig. 3. At a photon energy $h\nu < 1.75$ eV, the excited electrons

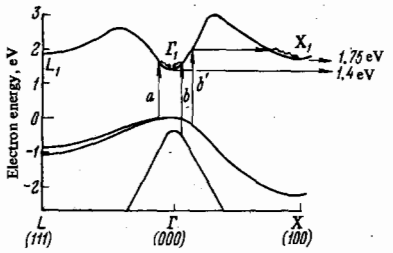

FIG. 3. The band structure of GaAs. a—Direct electronic transitions for $h\nu < 1.75$ eV; b—for $h\nu > 1.75$ eV.

are thermalized in the Γ_1 minimum of the lower conduction band. When $h\nu > 1.75$ eV, part of the electrons is excited to levels above the X_1 minimum, and are either thermalized into it, or are scattered from the X_1 minimum into the Γ_1 minimum. The distribution of optically excited electrons between the Γ_1 and X_1 minima can characterize the coefficients $F\Gamma$ and FX as functions of $h\nu$, and they are calculated from the band structure of GaAs. When $h\nu > 2.3$ eV, a considerable fraction of the electrons is excited near the surface (the absorption coefficient α is large here), and they escape into the vacuum as hot electrons.

Let us assume that we can neglect absorption of radiation in the band-bending region and in the surface film of cesium and that direct recombination of electrons from the X_1 minimum to the valence band does not occur. Then we can describe the motion of electrons thermalized in the two minima to the surface (along the z axis normal to the surface) with the following diffusion equations:

$$-D_\Gamma \frac{\partial^2 n_\Gamma}{\partial z^2} + \frac{n_\Gamma}{\tau_{\Gamma V}} = \frac{n_X}{\tau_{X\Gamma}} + J(1-R)F_\Gamma \alpha \exp(-\alpha z), \tag{4}$$

$$-D_X \frac{\partial^2 n_X}{\partial z^2} + \frac{n_X}{\tau_{X\Gamma}} = J(1-R)F_X \alpha \exp(-\alpha z). \tag{5}$$

Here z is the distance of the emitter from the surface, the D are the diffusion coefficients of Γ and X electrons, $\tau\Gamma V$ is the recombination lifetime of Γ electrons, and $\tau X\Gamma$ is the relaxation time for scattering of electrons from the X to the Γ minimum. The term $n_X/\tau_{X\Gamma}$ simultaneously determines the rate of generation of electrons in the Γ minimum by scattering from the X minimum and the rate of loss of electrons from the X minimum.

The term containing the exponential factor in both equations determines the rate of optical generation of electrons. J is the number of photons incident per unit surface of the emitter, and R is the coefficient of reflection of the material.

Simultaneous solution of these equations permits us to determine the flux density of electrons arriving at the boundary of the band-bending region. Upon introducing the factors P_X and $P\Gamma$, which characterize the probability of escape of electrons into the vacuum, we get the following expressions for the quantum yield of photoemission (i.e., the numbers of emitted electrons per incident photon):

$$Y_X = \frac{P_X F_X}{1+(1/\alpha L_X)}(1-R), \tag{6}$$

$$Y_\Gamma = (1-R)\frac{P_\Gamma}{1+(1/\alpha L_\Gamma)}\left\{F_\Gamma + \frac{F_X L_\Gamma}{\alpha L_X (L_\Gamma + L_X)[1+(1/\alpha L_X)]}\right\}. \tag{7}$$

Here $L = \sqrt{D\tau} = \sqrt{\mu\tau(kT/e)}$ is the diffusion length of the electrons.

We see from expressions (6) and (7) that one can get the largest quantum yield in an NEA-photocathode when

the diffusion length of the electrons is so large that it satisfies the inequality

$$\alpha L > 1 \tag{8}$$

while the probability of escape of the electrons at the surface $P \to 1$. In the limit, the quantum yield near the threshold of the photoeffect (Y_Γ) approaches $(1-R)P_\Gamma$. The diffusion length L_Γ of the minority carriers is a bulk property of the emitter material. Its size depends on the perfection of structure of the semiconductor, which is determined by its method of preparation. Everything that reduces the recombination time of electrons or lowers their mobility (extremely high doping levels, presence of contaminating impurities, lattice defects, dislocations, and precipitates) also reduces the diffusion length L_Γ. Thus, an increase in the acceptor concentration from 1×10^{19} to 4×10^{19} cm^{-3} decreases L_Γ from 1.6 to 1.0 μm.[14,20] The requirement of a high concentration of acceptors for lowering the Fermi level in the bulk and for decreasing the width of the band-bending region at the surface contradicts the requirement for a long diffusion length of electrons. Hence, an optimal doping level that permits a reasonable compromise between these parameters is chosen for each material.

In the first photoemitters based on single crystals of GaAs doped with zinc at concentrations $1-3\times10^{19}$ cm^{-3}, L_Γ was as much as 1.2–1.6 μm.[6,17,20] Increases in diffusion length have been gained in different ways: by perfecting the methods of growing single crystals or methods of preparing epitaxial GaAs films, by reducing the doping level with compensation for the widened band-bending region by a more substantial reduction in the work function, e.g., by coating the surface with an activated film instead of cesium. Such a film can be obtained by successive (or simultaneous) treatment with cesium and oxygen[8,15,23] or by using films of other compounds having high dipole moments, e.g., CsF, CsOH, etc.[11,12,13,21] In the best modern photocathodes based on GaAs doped with zinc at a concentration ~5 $\times10^{18}$ cm^{-3}, a diffusion length of electrons of as much as ~6 μm has been obtained.[30]

It has been possible to get larger diffusion lengths by using as the dopant in GaAs silicon, germanium, or manganese instead of zinc.[26,27] A value $L_\Gamma \sim 5-7$ μm has been obtained in epitaxial gallium arsenide doped with Ge at concentrations $5\times10^{17}-2\times10^{18}$ cm^{-3}.

The probability of escape of electrons from the surface of a photoemitter is determined by their scattering in the subsurface band-bending region and in the activating film that lowers the work function of the cathode. In order to increase P, one must reduce the width of the band-bending region, or as it were, the width of its "detrimental" portion (by more substantial reduction of the work function) and one must also use optimal activating coatings of small thickness. Reduction of the work function, i.e., increase in the difference $\mathcal{E}_g - e\varphi$ (the absolute value of the negative affinity) must have its reasonable limits, since the thermoemission of the photocathode increases with decreasing φ. Bell[18,19] has calculated all the possible components of the thermoemission current for a typical GaAs–Cs–O photocathode and other $A^{III}B^{V}$ compounds. The theoretical relationship that he got between the specific thermocurrent and the work function φ at the surface shows that the thermoemission of GaAs–Cs–O is insignificant at zero electron affinity ($10^{-19}-10^{-18}$ A/cm^2 under the crudest assumptions). However, it increases to $10^{-16}-10^{-15}$ A/cm^2 as the work function is reduced to 1.2 eV (although even here it remains at the level of the best ordinary modern photocathodes).

One can reduce the energy losses in the band-bending region by narrowing this region, not only by increasing the acceptor concentration N_A, but also by decreasing the amount of bending $\Delta\mathcal{E}$ of the bands, as determined by the position of the Fermi level with respect to the top of the valence band at the surface of the material. The width of the band-bending region, which must not substantially exceed the scattering length for hot electrons, is determined by the expression

$$w = \sqrt{\frac{2\epsilon\Delta\mathcal{E}}{eN_A}}. \tag{9}$$

where ϵ is the dielectric constant of the material, and $\Delta\mathcal{E}$ is the amount of bending of the bands, as determined by the distance from the top of the valence band to the Fermi level at the surface. The smaller $\Delta\mathcal{E}$ is, the smaller the doping level N_A that permits one to get the required value of w, on which the escape probability P of electrons depends.

A number of studies[35-40] has discussed the problem of the position of the Fermi level at the surface of GaAs. Measurement of the height of the Schottky barrier at the boundary of GaAs and a thick Cs film indicates stabilization of the Fermi level at a distance of ~0.6 eV[37] from the top of the valence band.

The density and distribution of surface levels that stabilize the Fermi level at the surface of gallium arsenide coated with an adsorbed film are determined by the nature, and perhaps the thickness, of the adsorbed film. Thus, a value of $\Delta\mathcal{E} \approx 0.45$ eV has been obtained for gallium arsenide covered with a monatomic layer of cesium.[39] Activation of photocathodes by successive treatment of the surface of the gallium arsenide with cesium and oxygen not only gives a smaller work function, but it also gives rise to less bending of bands than a monolayer of cesium does. The value of $\Delta\mathcal{E}$ is 0.25–0.3 eV for GaAs activated with a Cs–O film.

In[30], they studied the relation of the band bending to the crystallographic plane of GaAs activated with a Cs–O film. It turned out that the (110) face commonly used in single-crystal photocathodes is characterized by stabilization of the Fermi level at the surface covered with a Cs–O film at the distance $\Delta\mathcal{E} = 0.23$ eV, and the (100) face has the close-lying value $\Delta\mathcal{E} = 0.28$ eV. The (111A) face having Ga atoms at the surface shows a considerably greater band bending $\Delta\mathcal{E} = 0.86$ eV, while the (111B) face with As atoms at the surface has the smallest value $\Delta\mathcal{E} = 0.1$ eV.

In a specimen having a Zn impurity concentration ~5×10^{18} cm^{-3}, the width of the band-bending region at the surface of the (111A) and (111B) faces amounts to 155 and 51 Å, respectively, while the escape probabilities of electrons are 0.21 and 0.49 (and of the order of 0.3 for the (110) and (100) faces). The highest value ever measured of the integral sensitivity was obtained with a photocathode specimen prepared by activating a (111B) face of epitaxial GaAs with cesium and oxygen. It was 2060 μA/lumen (with an escape probability $P = 0.58$ and electron diffusion length $L = 6$ μm).

There are two conceptions on the role of the activating film on the surface of the GaAs, and in particular,

on the explanation of the nature and mechanism of action of the coating, as obtained by repeated alternate (or simultaneous) deposition on the surface of cesium and oxygen (up to 6–10 Cs–O layers): the heterojunction model and the polarized-dipole model. The heterojunction model[13,15,16,22,23,28,30] treats the surface layer as being a film of cesium oxide (assumed to be Cs_2O), and ascribes to it the bulk properties of this material, which is a broad-band electronic semiconductor ($\mathcal{E}_g$ = 2–2.2 eV) having a high donor concentration of ~10^{19} cm^{-3}, a small electron affinity $\mathcal{E}_a$ = 0.45 eV, and a low work function (which decreases with greater thickness of the Cs_2O film). According to the heterojunction theory, a potential barrier exists at the p-$A^{III}B^V$–n-Cs_2O boundary (a potential jump in the conduction band). The height of the barrier above the Fermi level is determined by the relationship between the electron affinities and the widths of the forbidden bands of the p- and n-type materials. In calculating the height of this barrier, one takes account of the fact that the Cs_2O film is deposited on a GaAs surface already treated with cesium, i.e., on a surface whose work function has already been reduced. An estimate of the minimum height of the intermediate barrier at the GaAs(Cs)–Cs_2O junction with account for tunneling of electrons through its upper part gives the value of 1.1 eV. Thus the intermediate barrier does not restrict the threshold for photoemission from GaAs. When one uses materials having narrower bands, GaSb or ternary $A^{III}B^V$ compounds, the photoeffect threshold is determined by the greatest of the three energies: the width $\mathcal{E}_g$ of the forbidden band, the height $\mathcal{E}_B$ of the intermediate barrier, or the work function $e\varphi$. Thus, in a study of materials having $\mathcal{E}_g < e\varphi$, lowering the work function shifted the photoeffect threshold toward longer wavelengths until the work function became smaller than $\mathcal{E}_B$. In agreement with this model, the existence of a heterojunction barrier that limits the photoemission threshold makes it impossible to prepare NEA photocathodes having thresholds $\lambda_0 > 1.2$–1.3 μm.

In agreement with the heterojunction model, one cannot shift the threshold to longer wavelengths solely by using semiconductor materials having narrower forbidden bands (and correspondingly having a smaller work function so as to maintain the condition $e\varphi < \mathcal{E}_g$). One must take measures for simultaneous lowering of the height of the intermediate barrier, e.g., by special treatment of the surface of the material before activation.[101] The critical nature of the thickness of the activating coating arises from the fact that, on the one hand, increase in thickness is accompanied by lowering the work function (owing to band bending in the Cs_2O layer), and on the other hand, the electrons that pass through this film into the vacuum lose more energy.

Doubts on the correctness of the heterojunction model were raised by a more exact estimate of the thickness of the activating film: as shown by Sommer's[24] measurements, which were carried out by chemical analysis instead of the previous estimates from the fluxes of the introduced amounts of Cs and O with assumed high sticking coefficients, the amounts of cesium and oxygen in the film proved to be practically independent of the number of treatment cycles, but corresponded approximately to one monolayer of cesium (~4×10^{14} cm^{-2}) and one monolayer of Cs_2O (4.5×10^{14} cm^{-2}). At this concentration, it is hardly appropriate to ascribe the bulk properties of the material to the cesium oxide.

In the polarized-dipole model, the greater reduction of the work function of the surface when oxygen is introduced into a cesium-treated specimen is attributed to formation of a double layer of charges and to the larger dipole moment of the combination GaAs–O–Cs compared with the combination GaAs–Cs.[41,42] This model is confirmed by experiments on an electronically-stimulated desorption of cesium from substrates not subjected and subjected to oxygen treatment.[43] Recent experiments on infrared photocathodes based on ternary $A^{III}B^V$ compounds[58–61] have shown that the assumed limitation of the threshold of the photoeffect by the height of the intermediate barrier of a heterojunction (~1.1 eV, independently of the width of the forbidden band of the substrate material) is apparently not confirmed: it was possible to use InAsP and InGaAs with a monolayer Cs–O coating to prepare photocathodes having a photoemission threshold $h\nu_0 = 0.9$ eV ($\lambda_0 = 1.4$ μm), which was limited only by the width of the forbidden band of the material. The lowered photoemission quantum yield observed here is attributed to a decrease in the escape probability P of the electrons, which apparently involves a decrease in the absolute value of the negative electron affinity.

While there is as yet no exact quantitative theory of the action of the activating coating, experiment shows that the nature of the surface structure that arises in activation and the potential diagram of the surface region apparently depend not only on the relationship between the energy constants of the substrate and coating materials, but also on the state of the surface of the semiconductor, and on the method of cleaning and treating it.

The state of the surface, the stability of this state, and the effect of various contaminants on the photoemission properties of NEA cathodes have been studied with various modern methods of surface analysis: mass spectrometry,[44] Auger spectroscopy,[45,46] the method of electron-stimulated desorption, and study of electron-reflection characteristics.[43] An infinitesimal surface contamination by carbon, which is not removed in the usual methods of thermal cleaning, has been shown to exert a harmful influence on the sensitivity of photocathodes (this implies that oil-less pumping means are needed). It has been shown that instability of photoemission (lowering of the quantum yield in the near-threshold region of the spectrum) involves instability of the surface activating film, due to desorption of cesium in a continuously pumped space or adsorption of residual gases in sealed devices. Here the escape probability P of the electrons decreases; the bulk properties (the diffusion length of electrons) hardly vary.[31]

We must note that, although a Cs–O activating coating is stabler than a monolayer of Cs, introduction of oxygen increases the desorption cross section of the cesium under electron bombardment. This implies that it seems expedient in preparing NEA secondary-electron emitters to limit the activation of the surface to cesium alone, rather than Cs–O.

Films of CsF, CsOH, BaO, etc., have also been used as activating coatings, instead of Cs-O.[11-13,21,28,53,56,65,69] In line with the fact that the activating film on the surface of NEA emitters must have a quite definite optimum thickness, a need has arisen for new, high-purity cesium sources with flux intensities that can be regulated and monitored. Most research centers have used for this purpose either molecular cesium sources with a guided flux, e.g., "channel" sources in the form of a

nickel tube filled with a mixture of cesium chromate and Si, or ion sources based on cesium aluminosilicates, impregnated with cesium carbonate, aluminum, or using surface ionization of Cs on a hot tungsten tube. The advantage of the ion sources is that they permit one to monitor the degree of covering of the surface from the size of the ion current.[47-49] To introduce a controllable amount of oxygen, one uses either flow regulators, which use diffusion of oxygen through a heated thin-walled silver tube, or thermal release of oxygen from higher oxides (MnO_2, BaO_2, etc.).

Practical realization of the principle of building electron emitters having a negative electron affinity and preparation of such photo- and secondary emitters in sealed devices became possible only because of a high level of technology, because of development of methods of preparing high-quality semiconductor materials with perfect crystal structure, development of methods of cleaning their surfaces and optimizing the means of activation, and also because of invention of commercial superhigh vacuum apparatus (one needs a vacuum no worse than 10^{-9} Torr to prepare NEA emitters).

Table I gives the fundamental information on experimental photocathodes based on gallium arsenide prepared by cleaving single crystals in a superhigh vacuum (Sec. a of Table I) and on commercial types of photocathodes prepared by using polycrystalline or epitaxial films of this material and cleaning the surface by brief radiation heating to a temperature close to the dissociation point of this compound (~650° C). As we see, optimization of the method of preparing the material, the doping level, and the surface activation has permitted gaining a mean level of integral sensitivity of gallium-arsenide photocathodes of ~1000 μA/lumen (with a thermal emission of $\sim 10^{-16}$ A/cm^2), even in sealed devices, with twice as high a sensitivity in experimental apparatus. Figure 4 shows the spectral characteristics of the first GaAs–Cs photocathode of Scheer and van Laar in 1965 (on a cleaved single crystal) and of two modern gallium-arsenide photocathodes, one being a cleaved GaAs(Zn)–Cs–O photocathode having a sensitivity of 1700 μA/lumen, and the other an epitaxial GaAs(Zn)–Cs–O photocathode (with a [111B] surface) with a sensitivity of 1837 μA/lumen.[38] The development of new ideas on the factors that affect the photoemission efficiency has facilitated in recent years a considerable refinement of ordinary photoemission materials. For comparison, Fig. 8 shows the characteristics of a standard (S-20) and a new modification (ERMA-III) of a multialkali photocathode. Figure 5 gives the spectral characteristics of two types of NEA-photocathodes used in commercial types of photo-

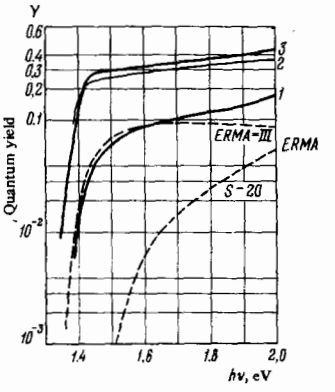

FIG. 4. Spectral characteristics of photocathodes. 1–GaAs-Cs[4]; 2–GaAs-Cs-O with a sensitivity of 1700 μA/lumen[101]; 3–GaAs-Cs-O (111B face) with a sensitivity of 1837 μA/lumen[30]. Dotted lines–the spectral characteristics of ordinary photocathodes: the S-20 multialkali cathode and the ERMA-III cathode with increased red sensitivity.

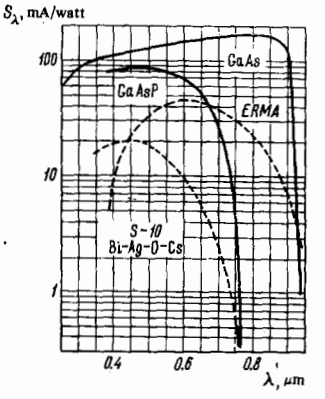

FIG. 5. Spectral characteristics of commercial NEA-photocathodes used in photomultipliers by the RCA firm. The dotted line shows the characteristics of standard photocathodes [101].

TABLE I. Fundamental Properties of Photoemitters Based on GaAs

Material	Dopant, cm^{-3}	Cleaning of surface	Activation	Integral sensitivity, μA/lumen	P		L		Reference
					Γ, μm	x, Å	Γ, μm	x, Å	
a) Single crystal (110)	Zn $4\cdot10^{19}$	Cleavage in ultrahigh vacuum	Cs	500	—	—	—	—	4
Single crystal (110)	Zn $2-6\cdot10^{19}$	Cleavage in ultrahigh vacuum	Cs—O	500	—	—	—	—	8
Single crystal (110)	Zn 10^{19}	Heating to 650°C	Cs—O	600	0.11	0.47	1.45	1000	17
Single crystal (110)	Zn $4\cdot10^{19}$	Cleavage	Cs+(O+Cs)[6]	1000	0.37	0.6	1.2	300	5
Single crystal (110)	Zn $2.6\cdot10^{18}$—$5\cdot10^{19}$	»	Cs—O	1100	0.45	0.5	1.38	1200	20
Single crystal (110)	Zn 10^{18} Si	»	CsF, Cs CsF	— 1240	0.5 —	— —	— —	— —	21 26
Single crystal (100)	Zn $5\cdot10^{18}$—$1\cdot10^{19}$	Heating	Cs—O	1700	0.55—0.6	1.2—3	—	—	104
Single crystal (111B)	Zn $5\cdot10^{18}$	»	Cs—O	2060	0.6	6	—	—	30
	Zn $5\cdot10^{19}$	»	Cs	220	—	—	—	—	64
b) Polycrystal (evap.) Vapor epitaxy	Zn $1.5\cdot10^{19}$	Ion bombardment	Cs—O	423	—	—	—	—	65
Epitaxy	Zn	Heating	Cs—O	500	—	—	—	—	24
Liquid epitaxy	Ge $5\cdot10^{17}$—$2\cdot10^{18}$	Heating	Cs—O	1100	—	5—7	—	—	27
Epitaxy	Zn	Heating	Cs—O	1000	—	—	—	—	33

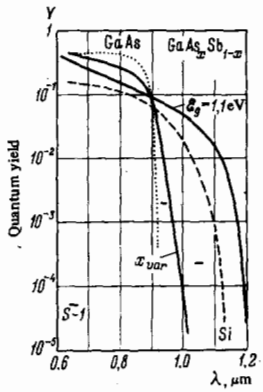

FIG. 6. Spectral characteristics of two photocathodes based on GaAsSb[57,104]. Dotted line—silicon NEA-photocathode[59]. The characteristic of a GaAs–Cs–O photocathode is given for comparison.

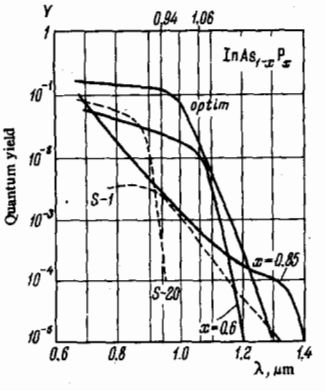

FIG. 7. Spectral characteristics of photocathodes based on InAsP[58,60].

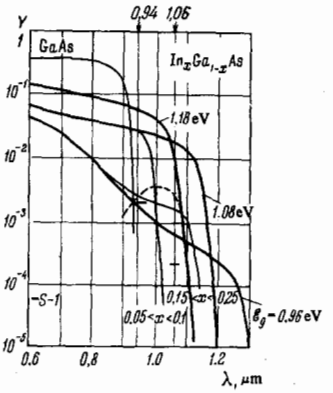

FIG. 8. Spectral characteristics of photochathodes based on InGaAs[61,104]. The dotted line shows the characteristic of a semitransparent photocathode of this composition[2].

multipliers by the RCA firm. As we see, the NEA photocathode has a high and uniform efficiency up to a wavelength $\lambda \sim 850$ nm, where the spectral sensitivity of the GaAs cathode exceeds 100 mA/W, while it is 15–20 mA/W in the best multialkali photocathodes. It is inferior to the multialkali photocathode only in the spectral range $\lambda > 900$ nm.

In order to prepare infrared-sensitive photocathodes, materials having narrower bands are used, mainly ternary $A^{III}B^{V}$ compounds, whose widths of forbidden bands can be smoothly varied by varying the ratio of components in the solid solution.[50-58,60-62] It was shown possible in 1970 to achieve a negative electron affinity in silicon.[59,84] Although silicon is distinguished by its very large minority-carrier diffusion length, it could hardly be classified as a promising material for preparing photocathodes: having indirect bands, silicon has a low optical absorption near the threshold. This leads to a smoother trend of the spectral characteristic in the near-threshold region. Silicon can be successfully used to prepare other types of NEA emitters, e.g., secondary or cold cathodes. As we have stated above, the shift of spectral characteristics to longer wavelengths as the width of the forbidden band of $A^{III}B^{V}$ decreases is accompanied by impairment of form and decrease in quantum yield.[2)] It has been possible to shift the photoemission threshold without substantially lowering the quantum yield by using films of $GaAs_xSb_{1-x}$ of variable composition, having a forbidden band that narrows smoothly in the direction toward the surface. Owing to the slope of the lower boundary of the conduction band, such films contain an internal field that facilitates transport of excited electrons to the surface.[57] Figure 6 shows the spectral characteristic of this cathode, as well as the characteristic of a homogeneous GaAsSb cathode having a forbidden-band width $\mathscr{E}_g = 1.1$ eV.[104] This same graph shows the spectral characteristic of an NEA photocathode made of silicon having the same width of forbidden band.[59]

The best results in making efficient photocathodes for the infrared have been obtained with the ternary compounds $InAs_{1-x}P_x$ and $In_xGa_{1-x}As$. Figure 7 shows the spectral characteristics of two photocathodes based on $InAs_{1-x}P_x$ ($x = 0.6$ and 0.85) according to [58], together with the envelope curve that shows the maximum sensitivity of photocathodes of this composition as optimized by varying x and the thickness of the activating coating for operation in this spectral region.[60] For comparison, the dotted lines show the spectral characteristics of a multialkali (S-20) and a silver-oxygen-cesium (S-1) photocathode. Figure 8 shows the spectral characteristics of several photocathodes based on $In_xGa_{1-x}As$. The

TABLE II. Fundamental Data on Infrared Photocathodes

Material	Activation	Integral sensitivity, μA/lumen	$\mathscr{E}_g$, $h\nu_0$, eV	Quantum yield Y: at 1.06 μm	at 0.94 μm	Reference
InP	Cs—O	450	1.24	—	—	50
$In_xGa_{1-x}As$ $x=0.11$	CsOH	245	1.16	—	—	51
$x=0.16$	Cs—O	—	—	$5\cdot10^{-3}$	10^{-2}	98
$x=0,25$	Cs—F	130	1.0	—	—	53
$x=0.3$	Cs—O	—	0,95	—	—	54
$x=0—0,22$	То же	—	1.4—1.08	$4\cdot10^{-4}$	$5.5\cdot10^{-2}$	62
$x=0,14—0.31$	» »	—	То 0.9	$2\cdot10^{-2}$	—	61
$InAs_xP_{1-x}$ $x=0.15$	» »	—	1.1	$8\cdot10^{-3}$	—	58
$x=0.15—0,4$	» »	—	То 0.9	$4\cdot10^{-3}$	—	58
$x=0—0.26$	» »	800	—	$2\cdot10^{-2}$	—	60
InAsP	» »	1126	1.05 (in a sealed device)	—	—	63
	» »	1300	1.1	—	—	60, 101
$GaAs_xSb_{1-x}$ (with variable x)	» »	700	1.06	$2\cdot10^{-3}$	—	57
Si	» »	—	1.1	—	—	59

thin lines refer to the cathodes in commercial sealed devices.[104]

The visible lack of a limitation of the photoemission threshold by an intermediate barrier (but with limitation only by the width of the forbidden band of the material) permits us to expect that we can shift the photoemission threshold as far as wavelengths of ~1.8 μm by further improvement of the quality of the used materials and means of activating them (in line with the actually attainable minimum work function ~0.7 eV). Table II gives the fundamental information on NEA photocathodes sensitive to the infrared.

The first reports of commercial production of photomultipliers having gallium arsenide (and gallium arsenide-phosphide for the visible spectrum) photocathodes appeared in 1969. The first devices with photocathodes sensitive to the infrared were already being produced in 1970, and they were designed for detecting infrared ra-

diation of light emitting diodes and lasers. For operation with light emitting diodes and injection lasers based on gallium arsenide ($\lambda = 930-950$ nm), one uses mainly photocathodes based on $In_xGa_{1-x}As$ ($0.05 < x < 0.10$). It has a spectral sensitivity in this spectral region of ~30–40 mA/W and a thermal emission that does not exceed 10^{-16} A/cm^2. At this wavelength, ordinary photocathodes, e.g., the S-20, have a spectral sensitivity of ~0.1 mA/W, and S-1 photocathodes have ~1–2 mA/W (and the latter have a thermal emission at least three orders of magnitude greater!). Photocathodes of the same composition optimized for operation in the region of Nd laser emission (1.06 μm) are characterized by a larger percentage of In ($0.15 < x < 0.25$). Their spectral sensitivity at 1.06 μm is as great as 15–17 mA/W (a quantum yield of ~2%). That is, it exceeds by a factor of several tens the sensitivity of the standard S-1 cathode, while the thermal emission amounts to only ~10^{15} A/cm^2.

On the practical level, the development of technologically feasible methods of preparing NEA photocathodes in the form of films is of greatest interest, and especially thin semitransparent films on transparent substrates for use as cathodes illuminated from the back ("transmission mode").

A series of studies has calculated[69-71] the optimum thickness of the photosensitive layer for getting the maximum sensitivity in illumination from the back and the relation of this sensitivity to the quality of the material (the diffusion length for electrons), to the defect density at the cathode-substrate boundary (the rate of surface recombination), and to the optical properties of the system (reflection at the cathode-vacuum and cathode-substrate boundaries). Analysis of the operation of a semitransparent GaAs photocathode shows that near the threshold of the photoeffect (up to $h\nu = 1.45-1.75$ eV) one can get a photoemission quantum yield that even exceeds the corresponding quantity in direct illumination with a thickness of photosensitive film not exceeding the diffusion length for electrons. However, a number of conditions must be satisfied (absence of lattice-mismatch defects at the cathode-substrate boundary, and optical coating of the illuminated surface). The spectral dependence of the quantum yield in illumination from the back has a maximum at a definite value of the product αL that depends on the thickness of the film (α is the optical absorption coefficient of the material).

In order to prepare semitransparent photocathodes, one needs high-quality materials not inferior in their bulk properties to the single crystals used in preparing good opaque cathodes. We can cite the following calculated relation.

A GaAs photocathode having $L = 1.6$ μm and $P = 0.37$ has at $h\nu = 1.5$ eV a direct-illumination quantum yield $Y = 0.139$. A semitransparent photocathode made of the same material with a film thickness of 1.2–1.6 μm can have a quantum yield ~0.144 in the absence of surface recombination without coating, or 0.216 when coated. However, if the diffusion length proves to be an order of magnitude shorter (0.16 μm), the quantum yield in backward illumination decreases by more than an order of magnitude, while it requires a considerable decrease in film thickness to optimize it. Owing to the small optical absorption coefficient near the photoemission threshold ($\alpha \sim 1$ μm^{-1} for GaAs), the diffusion length for electrons in semitransparent films must be greater than 1 μm. Preparation of thin tilms (of the order of 1 μm) that maintain a high quality of material presents great technical difficulties. One can get very thin films by vacuum sputtering (the three-temperature method)[67], but they are polycrystalline with a fine-grained structure and have a diffusion length of only several hundred Ångstroms.

Films having $L \leq 4000$ Å have been prepared by a modified cathode-sputtering method.[73] One gets the best quality of films by preparing them by the method of vapor-phase or liquid epitaxy, but starting only with a certain, not too small thickness. Liquid-phase epitaxy permits one to monitor exactly the stoichiometry, the degree of doping, and the structure of the films during the growth process,[66] but it requires a subsequent cleaning of the surface by etching. Vapor-phase epitaxy is the most practically-developed method, which does not require subsequent etching.

The need for a low defect density at the substrate-cathode boundary requires a careful choice of the substrate material. People have tried to use as substrates glass, fused or single-crystal sapphire, and silicon, which is transparent in thin films in the long-wavelength region.[74] In order to maintain good structure in the transverse direction (normal to the surface of the film), polycrystalline films were prepared with grain sizes equal to the film thickness (0.6–0.8 μm).[71] Even here, however, the sensitivity of the photocathodes in transmission remained more than an order of magnitude below that in direct illumination. It seems most promising to prepare epitaxial films on crystalline substrates having close-lying lattice parameters, i.e., on $A^{III}B^V$ compounds having wider forbidden bands. Semitransparent photocathodes have been described that are made of GaAsSb ($\mathcal{E}_g = 1.15$ eV) on a substrate made of chromium-doped gallium arsenide, which is transparent to 1.4 eV,[57] and of GaAs on an AlGaAs substrate.[75,93] The best results have been obtained with photocathodes made of InGaAs on substrates of GaAs andGaP.[62] We should note that substrates of this type serve as optical filters that restrict the sensitivity of the photocathodes in the short-wave region of the spectrum.

As the technology of preparing materials having great diffusion lengths for electrons is perfected, people will be able to solve the problem of making semitransparent photocathodes without substrates in the form of mechanically strong free films (plates) several microns thick.

Table III gives the fundamental information on experimental semitransparent photocathodes based on $A^{III}B^V$, and Fig. 9 shows the experimentally obtained spectral characteristics of these cathodes made of GaAs and of two types of ternary compounds based on GaAs.

Use of materials having negative electron affinity as secondary-electron emitters is facilitated by the fact that one can use for this purpose semiconductors having wider forbidden bands, and the conditions for negative affinity are satisfied at higher values of the work function than for photoemission. Consequently, secondary emitters are less sensitive to poorer vacuum. This made it possible to produce as early as 1968 photomultipliers having dynodes (or with a single first dynode) made of gallium phosphide ($\mathcal{E}_g = 2.3$ eV) activated with a cesium film. The great escape depth of

TABLE III. Fundamental Information on Semitransparent Photocathodes.

Material	Deposition method	Film thickness, μm	Substrate	Integral sensitivity, μA/lumen		Quantum yield, Y		hν, eV	Reference
				Reflection	Transmission	Reflection	Transmission		
GaAs(Zn)	Vapor epitaxy	2.5	Sapphire	100	1	$8\cdot10^{-4}$ $2\cdot10^{-3}$	10^{-3} 10^{-3}	1.4 1.5	68
GaAsSb	Liquid epitaxy	2.0	GaAs (Cr)	—	—	—	10^{-2}	1.37	69
GaAs	Vapor epitaxy	2.5—0,85	Sapphire	—	—	—	$6\cdot10^{-2}$	1.45	70
GaAs	Evap.	2.0	Glass, sapphire, quartz	—	10	—	$5\cdot10^{-3}$	3.0	67
GaAs	Vapor epitaxy	0.6—0.8	Sapphire	—	70	—	10^{-2}	1.7	71
GaAs	Evap.		Glass, sapphire, quartz	—	—	$3\cdot10^{-4}$	$3\cdot10^{-4}$	1.5	68
GaAs	Cathode sputtering	0.35—1.0	Singlecrystal sapphire	—	—	$2\cdot10^{-3}$ 10^{-1}	$2\cdot10^{-4}$ $2\cdot10^{-3}$	1.5 3.0	73
GaAs	Liquid epitaxy		Silicon	—	—	—	—	—	74
GaAs(Ge) InGaAs	Liquid epitaxy	10—13 0.1—1.0	AlGaAs GaAs, GaP	1000 —	— —	— $3\cdot10^{-3}$	— $3\cdot10^{-3}$	— 1.25	93 62

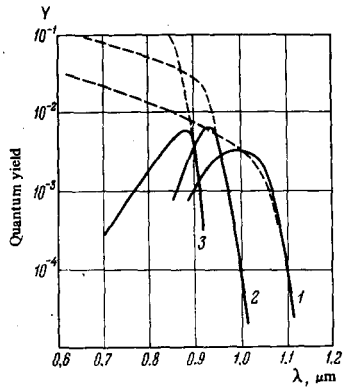

FIG. 9. Spectral characteristics of semitransparent photocathodes. 1—InGaAs on GaAs[2]; 2—GaAsSb on GaAs[69]; 3—GaAs (2.5 μm thick) on sapphire[70]. The dotted lines are the characteristics of the corresponding cathodes in direct illumination.

secondary electrons in NEA emitters gives rise to extremely high values of the secondary-emission coefficient (SEC) in the high-energy region of primary electrons. Thus, the calculated SEC (σ) of GaP—As at the maximum is $\sigma_m \sim 250$ at $U_p \sim 20$ kV.[76] At $U_p = 2.5$ kV, $\sigma = 130$ has actually been obtained, and $\sigma = 30-50$ at $U_p = 600$ V.[77-83] A secondary-emission coefficient ~400 has been obtained in epitaxial GaAs—Cs—O at $U_p = 20$ kV.[80] There is a report of a calculated value of $\sigma_m \sim 1000$ for this material.[81] The lack of any restriction by optical properties permits one to use more widely as secondary emitters materials having a great diffusion length, e.g., silicon, by preparing from them transmission secondary emitters in the form of free thin plates (films) without supporting grids. Figure 10 shows the emission characteristics of silicon activated with Cs—O upon electron bombardment of a plate 4—5 μm thick on the front ("reflection") and back ("transmission") sides.[84] It also shows the characteristics in reflection of the emitters GaP—Cs, GaP—Cs—O, and GaAs—Cs—O, and for comparison, one of the materials (Cs_3Sb) commonly used in photomultipliers. Apparently, the use of silicon diodes in photomultipliers will be hindered by their high thermal emission, which is as much as $\sim10^{-10}$ A/cm² at room temperature.[106] There is a description of a transmission secondary emitter based on GaP in the form of a film ~0.2 μm thick, epitaxially grown on GaAs with the substrate subsequently etched away. At $U_p = 2$ kV, the SEC of such emitters is as great as ~100.[78] In thin plates of GaAs (3—5 μm), people have obtained at $U_p = 10$ kV an SEC ~115 in reflection and up to 30 in transmission.[80]

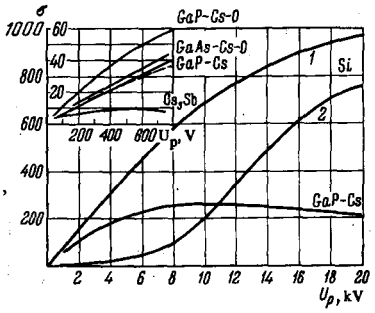

FIG. 10. Emission characteristics of secondary emitters. 1—Si—Cs—O is reflection, 2—in transmission[84], and GaP—Cs; above—emission characteristics in the region of low primary voltages for GaP—Cs[76,85], GaP—Cs—O[83], and GaAs—Cs—O[82]; the secondary-emission characteristic of Cs_3Sb is given for comparison.

Currently the American industry produces up to 40 types of photomultipliers having NEA emitters. Use of GaAs—Cs—O photocathodes with a mean integral sensitivity of ~1000 μA/lumen and thermal emission $\sim10^{-16}$ A/cm² in a photomultiplier permits a considerable improvement of their threshold characteristics, and it makes of these devices unique photodetectors that can detect single photons.[86] Use of first dynodes made of gallium phosphide with an amplification of ~50 instead of 3—5 substantially improves the statistics of the emission processes. This makes it possible to reduce the noise factor introduced by the dynode system from 0.25 for the best ordinary photomultipliers to 0.04. Thus the photomultiplier becomes an ideal device in which amplification is not accompanied by an increase in noise, and the sensitivity threshold is determined solely by the statistical fluctuations of the thermal emission of the photocathode. With slight cooling to −20° C, the dark current in these photomultipliers amounts to ~2 pulses per second.

The high amplification of the first dynode sharply improves the amplitude resolution of the photomultiplier. This is especially important in detecting very weak scintillations from low-energy radiation. The photomultipliers have a narrow electron distribution, with a half-width for a single-electron pulse of ~40%, and they permit one to distinguish clearly up to six electron peaks.

In line with the narrowing of the energy spectrum of the photo- and secondary electrons, the time resolution of the photomultipliers is also considerably improved. There is a report of an improvement of the time resolution of single-photon pulses by 40% as compared with the photomultipliers having copper-beryllium dynodes.[87] The RCA-C31024 photomultiplier having five dynodes made of GaP—Cs is characterized by a leading front of single-electron pulses of ~0.8 nsec and a pulse duration of ~1.5 nsec at an amplification of 10^8.[88] The most promising line of further improvement of the photomultiplier seems to be that of using transmission dynodes, which permit considerable improvement of the time resolution. Calculations[106] show that when one uses one transmission dynode made of GaAs with an amplification of ~100, one can get a duration of the leading front of ~37 nsec and a pulse half-width of ~135 nsec. Measurement of the service life of devices using GaP—Cs dynodes has shown that they are at least as stable as devices with the ordinary alloy dynodes.

The high secondary-emission coefficients render the new materials extremely promising also in use as targets for identification of particles at relativistic energies.[81]

The principle of negative electron affinity is fruitful, not only as applied to photo- and secondary electron

emitters, but also to other types of unheated electron emitters.

The possibility of using forward-biased surface-barrier and p–n junctions as injection cold cathodes has been studied intensively over the past 5–10 years. Discovery of the phenomenon of negative electron affinity has facilitated a sharp improvement in the parameters of this type of electron emitter as well. The principle of action of injection cold cathodes with negative electron affinity is that, when a forward bias is applied to a p–n junction having an outer p-layer, electrons are injected into the conduction band of the latter. They diffuse to the surface and escape into the vacuum if the thickness of the p-region does not exceed their diffusion length and there is no potential barrier at the surface. The electron-injection coefficient α is designated as the ratio of the number of electrons injected into the p-region to the total number of carriers (electrons and holes) that constitute the direct current across the junction. The fraction β of the injected electrons that arrive at the surface of the p-layer is determined by the relationship between the thickness of the p-layer and the diffusion length of the electrons. The escape probability P of these electrons into the vacuum depends on the same circumstances as in photo- and secondary emission from similar structures. The efficiency of a cold injection cathode, as defined as the ratio of the emission current to the current across the junction, is equal to the product of these quantities:

$$I_e/I_{p-n} = \alpha \cdot \beta \cdot P. \qquad (10)$$

The efficiency depends on the material that the cathode is made of, on the technical possibilities of producing an outer p-layer of small enough thickness (in practice, several micrometers), and on the treatment of the surface. Considerable difficulties are involved with the need to create current-carrying contacts that do not disturb the structure of the thin junction.

A cold injection cathode based on an epitaxial p–n junction in GaAs with a surface activated with cesium and oxygen was first made in 1969.[89] Its efficiency was low, mainly because of an unfortunate geometry: the emitting surface was a lateral section of the p–n junction. Subsequently, a flat, thinly deposited p–n junction in silicon was used for this purpose.[90] A note [90] reports on getting an efficiency of cold emission of ~2%, and a stable emission current of ~7.3 mA (at a current density of ~1 A/cm^2).

A number of foreign companies are vigorously involved in developing commercial injection cathodes. There are reports on preparation for sale of single and matrix p–n cathodes made of gallium phosphide, and on obtaining current densities up to several amperes per cm^2 in a steady-state mode, and more than 100 A/cm^2 in a pulsed mode.[91]

At the same time, a second variant of the negative-electron-affinity cold cathode has been developed: the optoelectronic cathode, in which optical excitation of electrons in the outer p-layer is used instead of injection into it, as the radiation of a light diode is absorbed in it. The optoelectronic cathode is a combination of an electrically controlled light source with a semitransparent photocathode. The efficiency of an optoelectronic cathode, i.e., the ratio of the emission current to the light-diode current, is determined by the product of the quantum efficiency of the light diode, the transfer coefficient of the radiation to the light-sensitive layer, the absorption of radiation in it, and the quantum yield of photoemission in the spectral region of emission of the light diode.

The appearance of gallium arsenide photocathodes having negative electron affinity immediately stimulated the invention of optoelectronic cold cathodes in which a semitransparent GaAs–Cs–O photoemitter had been directly deposited (with direct optical contact) on the emitting p-region of the light diode. The emission of the light diode occurs at a quantum energy somewhat smaller than the width of the forbidden band of the material. Hence, one chooses as the light-diode material an $A^{III}B^{V}$ semiconductor having a width of forbidden band slightly exceeding the width of the forbidden band of GaAs, e.g., AlGaAs having low Al content (at the same time, this makes it possible to grow high-quality epitaxial GaAs films on its surface). With a forward bias on the p–n junction in the AlGaAs, electrons are injected into the p-region, where they radiatively recombine. The radiation ($h\nu = 1.4–1.6$ eV) is absorbed in the p^+ layer of the GaAs grown on the p-region of the light diode. The generated photoelectrons diffuse to the surface, and they escape into the vacuum without substantial losses if the p-GaAs layer has the optimum thickness for a semitransparent photocathode.

The efficiency of the first cold cathodes of this type amounted to ~10^{-3}. This was explained mainly by insufficient sensitivity of the thin (~1 μm) semitransparent photocathode.[92] The design and means of preparing optoelectronic cathodes have subsequently been refined: a photosensitive layer made of high-quality gallium arsenide doped with germanium was deposited by liquid-phase epitaxy, and it had a thickness of 10–13 μm, which permitted more complete absorption of the radiation. The surface of the GaAs was activated by cesium and oxygen until maximum photosensitivity had been attained, being 700–1000 μA/lumen.[93] Figure 11 shows the structures of an injection cathode made of Si and of an optoelectronic cold cathode made of GaAs having a working surface of ~10^{-2} cm^2. The ohmic contact with the n-region was made with In, and that with the p-region was made with a pressure point contact. The efficiency of the optoelectronic cathode was as much as 1.6–2%, and the pulse current density as much as 3 A/cm^2. An approximate estimate of the theoretical limit of the efficiency when the thickness of the photosensitive layer is optimized, and with an internal quantum efficiency of the light diode of ~50%, gives a value of ~4%, if the escape probability of electrons is ~0.15.

As a number of technological problems are solved, mainly involving the technique of creating contacts, and with further increase in the emission current density, cold cathodes of both types may successfully replace

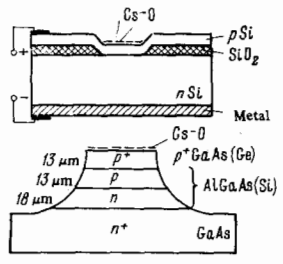

FIG. 11. Design of an injection cold cathode based on silicon[90] and of an optoelectronic cold cathode[93].

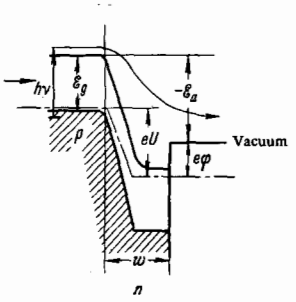

FIG. 12. Diagram of the photoemission of a reverse-biased p-n juntion through the thin outer n-region[94].

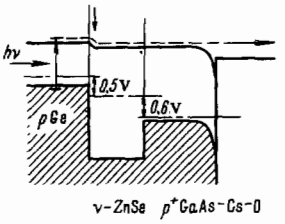

FIG. 13. Energy diagram of an externally-biased three-layer cathode structure[97].

thermoelectronic cathodes in a number of electronic devices. These emitters are of especial interest for electron-ray devices, in particular, for creating many-beam projectors with independent control of the beams.

In closing the review, I might also mention a number of as yet not achieved projects to invent efficient photocathodes having emission stimulated by an electric field in which conditions of negative electron affinity are also used. The idea is known of using the strong electric field that arises in the depleted region of a reverse-biased p–n junction for heating of electrons that have been optically excited in the p region in order to facilitate their escape through the surface potential barrier. Applying a reverse bias to a p–n junction having an outer n-region lowers the vacuum level with respect to the bottom of the conduction band of the p region, and it can give rise to a pattern analogous to the conditions of negative electron affinity. As we see in Fig. 12, the electron affinity for electrons excited in the p-region is defined by the expression

$$\mathcal{E}_a = e\varphi - \mathcal{E}_g - eU. \qquad (11)$$

In order to produce such photocathodes, one must create structures having very sharp p–n junctions, with a thickness of the n-region comparable with the phonon-scattering length of hot electrons. The problem is discussed in[94] of choosing optimal materials for building this type of photoemitters that are sensitive farther into the infrared than the existing NEA photocathodes are. The fundamental criterion is a small width of forbidden band, a large phonon scattering length of hot electrons, and the possibility of creating a strong enough field at the junction without having a tunnel current and avalanche breakdown. By using an approximate quantitative estimate of the parameters of the transitions, it has been shown possible to create p–n photoemitters based on InAs. This requires creating an n-type surface layer with a donor concentration of $\sim 10^{15}$ cm^{-3} and a thickness of ~0.6–0.8 μm. One must create a very thin n^+-layer activated with Cs and O to reduce the work function in order to permit contact with the surface of the n-region. The possibility of making photoemitters based on materials having even narrower bands, InSb and HgCdTe, has been discussed.

Patent descriptions exist on photoemitters of this type based on a Ge–GaP heterojunction and silicon.[95,96] In order to create a sharp fine-scale p–n junction on the surface of a p-Si plate, it has been proposed to use the method of ion implantation by 5–10 keV cesium ions, which become implanted to a depth of 50–200 Å. The surface is activated with slow Cs ions to reduce the work function. An annular diffusional n-region provides for contact with the outer layer of the cathode.

The principle of action of an infrared photocathode having two heterojunctions (with a transistor structure) has been discussed in [97] for the system p-Ge–ν-ZnSe–p^+-GaAs·(Cs–O) having a surface activated to the point of negative electron affinity. Figure 13 shows the energy diagram of this structure with an applied external bias. In essence, this system is a combination of an illuminated, reversed-biased junction and an outer emitter junction through which electrons are injected from the basis into the p-type gallium arsenide. The outer layer is an NEA photocathode in which optical excitation has been replaced by injection. The electrons that are excited by infrared radiation in the intrinsic band of the germanium (upon illumination from the substrate side) diffuse through the thin base (ZnSe), are injected into the GaAs, and escape into the vacuum, provided that the thickness of the GaAs layer does not exceed their diffusion length. The components of the three-layer structure were chosen with account taken of the idea that no potential jump (barrier) should arise in the conduction band at the boundaries of the two heterojunctions. The large width of the forbidden band of the base material (ZnSe) hinders the flow of a large hole current through the emitter junction.

There is as yet no information on the practical realization of photoemitters having an externally biased junction. To prepare them involves the great difficulty of producing structures having an extremely thin outer junction region (a fraction of a micron) with sufficient conductivity to ensure contact.

More than 100 original studies and several reviews[48-106] already have been concerned with describing the new class of efficient electron emitters and solving the problems that arise in preparing them. The rapid refinement of the parameters of the new emitters reveals the great interest of industry in producing devices having emitters that permit one to take a qualitative jump in an entire series of very important properties of these devices. The scientific value of the idea of producing and using negative electron affinity is unquestionable: the creation of a broad class of various emitters with negative electron affinity is one of the very great achievements of physical electronics throughout its history of existence.

[1)]The electron affinity $\mathcal{E}_a$ of a semiconductor is taken to be the energy spacing from the bottom of the conduction band to the vacuum level, which determines the height of the potential barrier for conduction electrons.

[2)]One of the reasons for this can be simply the increase in density of crystal-lattice defects as the percent composition of the narrow-band component of the compound increases.

[1]W. E. Spicer, Phys. Rev. **112**, 114 (1958); J. Appl. Phys. **31**, 2077 (1960).
[2]W. E. Spicer, A. H. Sommer, Photoelectronic Materials and Devices. Ed. S. Larach, 1965.
[3]A. H. Sommer, Photoemissive Materials, 1968.
[4]J. J. Scheer and J. van Laar, Solid State Comm. **3**, 189 (1965); West German Patent cl. 21d 29/20, No. 1256808, Dec. 2, 1954.
[5]J. W. James, J. L. Moll, and W. E. Spicer, Gallium

Arsenide. Proc. 2nd Intern. Symposium, 1968.
[6]L. W. James, J. L. Moll, Phys. Rev. 183, 749 (1969).
[7]R. C. Eden, J. L. Moll, and W. E. Spicer, Phys. Rev. Lett. 18, 597 (1967).
[8]A. A. Turnbull and G. B. Evans, J. Phys. D1, 155 (1968); Electronics 40, 234 (1967); British Patent (H 01 j 9/12) No. 1200899, Aug. 30, 1967.
[9]T. E. Fisher, Surface Sci. 10, 474 (1968).
[10]H. Sonnenberg and R. T. McKenzie, IEEE Trans. ED-15, 419 (1968).
[11]P. G. Borzyak, Yu. G. Zav'yalov, G. A. Katrich, and O. G. Sarbeĭ, Ukr. Fiz. Zh. 14, 403 (1969).
[12]M. Hagino and R. Nishida, Japanese J. Appl. Phys. 8, 123 (1969).
[13]H. Sonnenberg, Japan J. Appl. Phys. 8, 806 (1969).
[14]H. Sonnenberg, J. Appl. Phys. 40, 3414 (1969).
[15]H. Sonnenberg, Appl. Phys. Lett. 14, 289 (1969).
[16]H. Sonnenberg, Bull. Am. Phys. Soc. 14, 791 (1969); Appl. Phys. Lett. 21, 103, 278 (1972).
[17]Y.-Z. Liu, J. L. Moll, and W. E. Spicer, Appl. Phys. Lett. 14, 275 (1969).
[18]R. L. Bell, Sol. St. Electron. 12, 475 (1969).
[19]R. L. Bell, Sol. St. Electron. 13, 397 (1970).
[20]S. Garbe, Sol. St. Electron. 12, 893 (1969).
[21]S. Garbe, Phys. Stat. Sol. 2, 497 (1970).
[22]J. J. Uebbing, L. W. James, J. Appl. Phys. 41, 4505 (1970).
[23]L. W. James and J. J. Uebbing, Appl. Phys. Lett. 16, 370 (1970).
[24]A. H. Sommer, H. H. Whitaker, and B. F. Williams, Appl. Phys. Lett. 17, 273 (1970).
[25]A. H. Sommer, J. Appl. Phys. 42, 2158 (1971).
[26]S. Garbe, G. Frank, Gallium Arsenide and Related Compounds, London, 1970; Proc. Intern. Conference on GaAs, Aachen, 1970.
[27]H. Schade, H. Nelson, and H. Kressel, Appl. Phys. Lett. 18, 121 (1971).
[28]A. F. Milton and A. D. Baer, J. Appl. Phys. 42, 5095 (1971).
[29]J. M. Chen, Surf. Sci. 25, 457 (1971).
[30]L. W. James, G. A. Antypas, J. Edgecumbe, R. L. Moon, and R. L. Bell, J. Appl. Phys. 42, 4976 (1971).
[31]E. M. Yee, and D. A. Jackson, Sol. St. Electron. 15, 245 (1972).
[32]G. A. Allen, J. Phys. D4, 308 (1971).
[33]RCA advertisement, Appl. Optics 10, No. 7, A19 (1971) (photomultiplier with a GaAs cathode).
[34]A. A. Mead, Sol. St. Electron 9, 1023 (1966).
[35]J. J. Scheer and J. van Laar, Sol. St. Comm. 5, 303 (1967).
[36]J. Van Laar and J. J. Scheer, Surf. Sci. 8, 342 (1967).
[37]J. J. Uebbing, and R. L. Bell, Appl. Phys. Lett. 11, 357 (1967).
[38]J. van Laar and J. J. Scheer, Philips Techn. Rev. 29, 54 (1968).
[39]J. J. Scheer and J. van Laar, Surface Sci. 18, 130 (1969).
[40]W. Mönch, Surf. Sci. 21, 443 (1970).
[41]L. W. Swanson and R. W. Strayer, J. Chem. Phys. 48, 2421 (1968); B. E. Evans, L. W. Swanson and A. E. Bell, Surf. Sci. 11, 1 (1968).
[42]J. M. Chen, J. Appl. Phys. 41, 5008 (1970).
[43]T. E. Madey and J. T. Yates, J. Vac. Sci. Techn. 8, 39, 525 (1971).
[44]W. Klein, Bull. Am. Phys. Soc. 14, 854 (1969).
[45]J. J. Uebbing and N. J. Taylor, Bull. Am. Phys. Soc. 14, 792 (1969); N. J. Taylor, Vacuum 19, 575 (1969); J. J. Uebbing, J. Appl. Phys. 41, 802, 804 (1970); J. Vac. Sci. Techn. 7, 81 (1970).
[46]D. J. Miller and D. Haneman, Surf. Sci. 19, 45 (1970).
[47]H. M. Love and H. D. Wiederick, J. Phys. E2, 1091 (1969).
[48]D. L. Schaefer, Rev. Sci. Instr. 41, 274 (1970).
[49]W. Klein, Rev. Sci. Instr. 42, 1082 (1971).
[50]R. L. Bell and J. J. Uebbing, Appl. Phys. Lett. 12, 76 (1968); R. L. Bell, U.S. Patent No. 60144/68, Ser. No. 1258917 (Cs_2O on InP); British Patent (HOIj 1/34) No. 1258918 (InAsP).
[51]J. J. Uebbing and R. L. Bell, Proc. IEEE 56, 1624 (1968).
[52]D. L. Schaefer, J. Appl. Phys. 40, 445 (1969).
[53]W. Klein, J. Appl. Phys. 40, 4384 (1969); Bull. Am. Phys. Soc. 14, 791, 855 (1969).
[54]B. F. Williams, Appl. Phys. Lett. 14, 273 (1969).
[55]R. E. Simon, A. H. Sommer, J. J. Tietjen, and B. F. Williams, Appl. Phys. Lett. 15, 43 (1969); R. E. Simon, B. F. Williams, and R. Wasserman, British Patent (HOI j 1(32)) No. 1233721 (GaAsP).
[56]S. Garbe, Phys. St. Sol. 33, K87 (1969).
[57]G. A. Antypas and L. W. James, J. Appl. Phys. 41, 2165 (1970).
[58]H. Sonnenberg, Appl. Phys. Lett. 16, 245 (1970); 19, 431 (1971).
[59]R. U. Martinelli, Appl. Phys. Lett. 16, 261 (1970).
[60]L. W. James, G. A. Antypas, J. J. Uebbing, T. O. Yep, R. L. Bell, J. Appl. Phys. 42, 580 (1971).
[61]D. G. Fisher, R. E. Enstrom, and B. F. Williams, Appl. Phys. Lett. 18, 371 (1971).
[62]D. G. Fisher, R. E. Enstrom, J. S. Escher, and B. F. Williams, J. Appl. Phys. 43, 3815 (1972).
[63]R. L. Bell, L. W. James, G. A. Antypas, J. Edgecumbe, and R. L. Moon, Appl. Phys. Lett. 19, 513 (1971).
[64]R. F. Steinberg, Appl. Phys. Lett. 12, 63 (1968).
[65]S. Garbe and G. Frank, Sol. St. Comm. 7, 615 (1969).
[66]B. J. Stocker, M. J. Plummer and A. A. Turnbull, J. Phys. D3, 1299 (1970).
[67]T. Yasar, R. F. Steinberg, J. Vac. Sci. Techn. 6, 905 (1969); 7, 139 (1970).
[68]Syms, CHA Adv. Electron. El. Phys. 28a, 406 (1969); British Patent (HOI j 9/12) No. 1193002, May 28, 1970.
[69]G. A. Antypas, L. W. James, and J. J. Uebbing, J. Appl. Phys. 41, 2888 (1970).
[70]Y. Z. Liu, J. L. Moll, and W. E. Spicer, Appl. Phys. Lett. 17, 60 (1970).
[71]D. Andrew, J. P. Gowers, J. A. Henderson, M. J. Plummer, B. J. Stocker, and A. A. Turnbull, J. Phys. D3, 320 (1970).
[72]see Ref. 32.
[73]S. B. Hyder, J. Vac. Sci. Techn. 8, 228 (1971).
[74]J. C. Word, U.S. Patent cl. 313-95 (HOI j 39/18) No. 3575628, Nov. 26, 1968 (GaAs on Si).
[75]P. R. Selway, British Patent cl. HID (HOI j 1/34) No. 1239893, Mar. 5, 1970 (GaAs on AlGaAs).
[76]R. E. Simon and B. J. Williams, IEEE Trans. NS-15, 167 (1968).
[77]R. E. Simon, A. H. Sommer, J. J. Tietjen, and B. F. Williams, Appl. Phys. Lett. 13, 355 (1968).
[78]R. E. Simon, B. F. Williams, and R. Wasserman, U.S. Patent cl. 250-207 (HOI j) No. 3478213, Sep. 5, 1967, Nov. 11, 1969.
[79]G. A. Morton, H. M. Smith, and H. R. Krall, Appl. Phys. Lett. 13, 356 (1968); IEEE Trans. NS-16, 92 (1969).
[80]W. A. Gutierrez, H. D. Pommerrenig and S. L. Holt,

Appl. Phys. Lett. **21**, 249 (1972).
[81]J. Llacer, IEEE Trans. NS-17, 29 (1970); Bull. Am. Phys. Soc. **14**, 854 (1969).
[82]L. F. Afonina, A. I. Klimin, and G. B. Stuchinskiĭ, Élektron. Tekhn. **4**, 64 (1970).
[83]L. F. Afonina, V. M. Lagodinskiĭ, and G. B. Stuchinskiĭ, Izv. AN SSSR, Ser. Fiz. **35**, 1046 (1971).
[84]R. U. Martinelli, Appl. Phys. Lett. 17, 313 (1970).
[85]P. B. Coates, J. Phys. D7, L25 (1970).
[86]Canad. El. Eng. **12**, 31, 32 (1968); 13, 9 (1969) (photomultiplier with GaP dynodes); Phys. Today **23**, (10) 21 (1970).
[87]G. Present and D. B. Scral, Rev. Sci. Instr. **41**, 771 (1970).
[88]H. R. Krall, F. A. Helvy, and D. E. Persyk, IEEE Trans. NS-17, 71 (1970).
[89]B. F. Williams and R. E. Simon, Appl. Phys. Lett. **14**, 214 (1969).
[90]E. S. Kohn, Appl. Phys. Lett. 18, 272 (1971).
[91]Electronics **44**, 29 (1971); Sol. St. Technol. 14, 35 (1971).
[92]H. Kressel, E. S. Kohn, H. Nelson, J. J. Tietjen, and L. R. Weisberg, Appl. Phys. Lett. **16**, 359 (1970); Electronics **43**, 45 (1970).
[93]H. Schade, H. Nelson, and H. Kressel, Appl. Phys. Lett. **18**, 413 (1971).
[94]V. L. Dalal, J. Appl. Phys. **43**, 1160 (1972).
[95]S. A. Ward, U.S. Patent cl. HOI (j, 7/54) No. 3591424, Jun. 26, 1969, Jul. 6, 1971.
[96]B. V. Dore and D. V. Geppert, U.S. Patent cl. 313-94 No. 3408521, Nov. **22**, 1965, Oct. 29, 1968.
[97]A. G. Milnes and D. L. Feucht, Appl. Phys. Lett. **19**, 383 (1971).
[98]E. D. Savoy and J. J. Tietjen, Laser Focus **6**, 34 (1970).
[99]H. Sonnenberg, IEEE J. Sol. St. Circ. 5, 272 (1970).
[100]N. A. Soboleva, Éffektivnye fotoemittery (Efficient Photoemitters), VINITI (deposited document), 1970.
[101]R. L. Bell and W. E. Spicer, Proc. IEEE **58**, 1788 (1970).
[102]N. N. Petrov, Zh. Tekh. Fiz. **41**, 2473 (1971) [Sov. Phys.-Tech. Phys. **16**, 1965 (1972)].
[103]L. Eckertová, V. Starý, Výzkumné zprávo, 1971.
[104]B. F. Williams, J. J. Tietjen, Proc. IEEE **59**, 1489 (1971).
[105]M. Jedlička, Slaloproudý obzor **33**, 44 (1972).
[106]B. F. Williams, IEEE Trans. NS-19, 39 (1972).

Translated by M. V. King